



Innovation in assessment of the geothermal energy potential of abandoned hydrocarbon wells in the southern and southeastern foreground of the Bükk Mountains, northeast Hungary

Péter Szűcs^{1,2} · Endre Turai¹ · Viktor Mádai¹ · Péter Vass¹ · Rita Miklós¹ · Balázs Zákányi¹ · Csaba Ilyés^{1,2} · Zsombor Fekete¹ · Roland Kilik¹ · Ferenc Móricz¹ · Gábor Nyiri¹ · Marcell Szilvási¹ · Norbert Péter Szabó^{1,2}

Received: 8 December 2021 / Accepted: 19 October 2022 / Published online: 14 November 2022

© The Author(s) 2022

Abstract

An innovative methodology is introduced to study abandoned oil exploration drillings for possible geothermal energy production at a test area in northeast Hungary. An evaluation method supported by robust statistical analysis was elaborated to provide the possible future investors with adequate technical and earth-science related information for their decision-making processes. All the available data of 161 abandoned hydrocarbon wells, with different physical conditions, were examined based on the proposed evaluation system to provide information about the geothermal energy potential for each well, as well as over a bigger area. The abandoned wells and their environments, the quantity of stored heat, and the fluid temperature and geothermal heat were the key parameters determined, which are critical when considering geothermal energy utilization or thermal water production. The maximum amount of stored energy was determined as the sum of the amount of energy extractable from the rock and the fluid. The heat stored in the rock was determined by basin modelling. The evaluation process, using one-dimensional (1D) basin modelling and 3D lithological-stratigraphic modelling, was successfully applied in the pilot area. The maximum amount of heat stored in the fluid can be determined by subtracting the heat stored in the rock from the total heat. Drilling and completing geothermal wells are rather expensive in Hungary, depending on the depth and the types of geological formations. The application of this research could greatly reduce the cost and risk of creating new geothermal energy systems based on production wells or abandoned wells in Hungary or elsewhere.

Keywords Abandoned well · Geothermal energy potential · Thermal conditions · Groundwater statistics · Hungary

Introduction

There are natural geothermal conditions in the whole Carpathian Basin, which includes territory in Hungary (Boldizsár 1967). Szűcs and Madarász (2013) describe the major challenges associated with the utilization of the Hungarian deep thermal water resources and geothermal energy. The petroleum industry and the intense exploration activity since the 1960s have been providing a lot of geoscience-related information about the deep geological formations

and the heat flow properties that facilitate the utilization of geothermal energy in Hungary (Szanyi and Kovács 2010). It is also important to mention that, due to the intense petroleum exploration campaign over several decades, there are thousands of abandoned wells with different technical conditions in the country (Buday et al. 2015). In 2016, the University of Miskolc (Hungary) initiated the so-called PULSE national research project, for which the main objectives aim to meet the targets given by the National Energy Strategy (MND 2012). As part of the project, the possibility of active utilization of unproductive and abandoned wells was studied. At the beginning of the research, a special database of the unproductive and abandoned hydrocarbon extraction wells in Hungary was built and a suitable method was developed to find possible uses for these wells in the field of geothermal energy utilization.

The general concept of utilization of hydrocarbon wells for geothermal energy seems feasible because of the

✉ Norbert Péter Szabó
gfnmail@uni-miskolc.hu

¹ Faculty of Earth Science and Engineering, University of Miskolc, Miskolc-Egyetemváros 3515, Hungary

² MTA-ME Geoen지니어ing Research Group, Miskolc-Egyetemváros 3515, Hungary

naturally (high) temperature range (65–150 °C) of the produced fluids in the oil fields (Davis and Michaelides 2009; Kai et al. 2018; Liu et al. 2018; Templeton et al. 2014). In spite of there being a clear theoretical advantage to this use of hydrocarbon wells, only a few good examples are known internationally. Several geothermal power plants have been installed in oil fields across the world, using binary cycle systems, making the direct utilization of geothermal energy from petroleum wells a very promising research topic (Xianbiao et al. 2012). Two recent papers—Wang et al. (2018); Liu et al. (2018)—give several examples of facilities that are being operated already. In Hungary, the first large-scale research program dealing with the utilization of abandoned oil wells to produce electricity was launched in 1995 by the biggest national oil company (Árpási et al. 1997). As a continuation of this project, the first pilot geothermal power plant was to be installed in Iklódbördőce, Zala County, West Hungary. This important pilot project included the modification of two abandoned hydrocarbon extraction wells (Bobok and Tóth 2007)—one for the thermal water extraction and one for the reinjection process. Unfortunately, because of the low thermal water yield, the project was not completed (Tóth 2017). In this paper, a similar but much more complex study is undertaken in order to determine the geothermal energy potential of the investigated wells in a promising new area in the Bükk Mountains region, northeast Hungary.

Materials and Methods

Geothermal conditions in North Hungary

The two major geographic landscapes in northeast Hungary are the North Hungarian Mountains (NHM) and the Great Hungarian Plane (GHP) (Szűcs 2017). The pre-Neogene basement is covered by sediments in the GHP with depths reaching 7000 m. However, in the NHM, the pre-Neogene, pre-Cenozoic rocks are outcropping and form parts of the mountain range. Miocene volcanic rocks are the most widespread in mountainous areas. The geology of the great plain region and the mountainous area is rather complex (Haás 2013). The basement formations include a variety of Mesozoic (carbonates, shallow and deep-sea sediments), Paleozoic (siliciclastic and metamorphic rocks) and older (mainly metamorphic) rocks. Unfortunately, the basement rocks are still unidentified in large areas. The southeast border of this region overlaps the Mid-Hungarian fault zone, which divides the Alcapa and the Tisia plates. Another significant tectonic feature, the Darnó zone (SW–NE), runs through the area at the northwest border of the Bükk Mountains. The Cenozoic sediments in the basement have a wide range of thicknesses. The deepest part of the basement can reach more than 5,000 m in the region.

The pilot area was delineated (Fig. 1) based on preliminary evaluations. The thickness of Neogene sediments in the pilot area increases significantly from northwest to southeast, the bottom of it reaching 4,500 m below the sea level and in some areas even below 5,000 m. The central area is characterized by a series of depressions (at a depth of 3,000–3,500 m). The Neogene sediments are mainly composed of river sediments (e.g., gravel, sand, clay, loess).

Miocene acidic tuffs (rhyolite, dacite and rhyodacite rocks) are present on the surface of the investigated area (Pelikán 2005). Broadly speaking, Hungary can be characterized by a naturally high geothermal gradient (ca. 50 °C/km) due to the relatively thin crust under the area of the country. The spatial distribution of the geothermal gradient values reflects well the geologic structure of Hungary. The investigated area is characterized by high geothermal gradient values between 55 and 70 °C/km. The heat-flow values at the investigated area vary between 75 and 105 mW/m², which can also be considered suitable for geothermal energy exploitation. The rock temperature under such conditions may range between 60 and 75 °C at 1,000 m depth and 100–125 °C at 2,000 m depth (Dövényi et al. 1983). Although a few wells had been drilled at the beginning of the 20th century, the large-scale exploration activity was not started until the 1950s. The majority of the completed wells are hydrocarbon exploration wells. Exploration specifically for thermal water resources increased from the middle of the last century but has expanded greatly in the last two decades (Miklós et al. 2020).

Building a database of the investigated area

The first step of the conducted research involved the collection of data and the building of a database of the abandoned and unproductive hydrocarbon wells at the test site that have theoretical potential for geothermal energy use. The database included three main sources:

- A geothermal survey of Hungary (Tóth 2016)
- A database of unproductive hydrocarbon wells for the Bükk Mountains region developed from the original drilling and testing reports
- A cadaster of Hungarian thermal water wells (VITUKI 1994; MFGI 2015)

The geothermal survey of Hungary summarizes the basic data (i.e., name, identification code, coordinates, depth and year of construction, bottom of the hole and wellhead temperature) of nearly 2,000 thermal water wells located across the country. Around 1,500 wells were originally drilled for geothermal energy utilization and the others were completed for hydrocarbon exploration or extraction. All of them can be considered to have potential for geothermal use. The

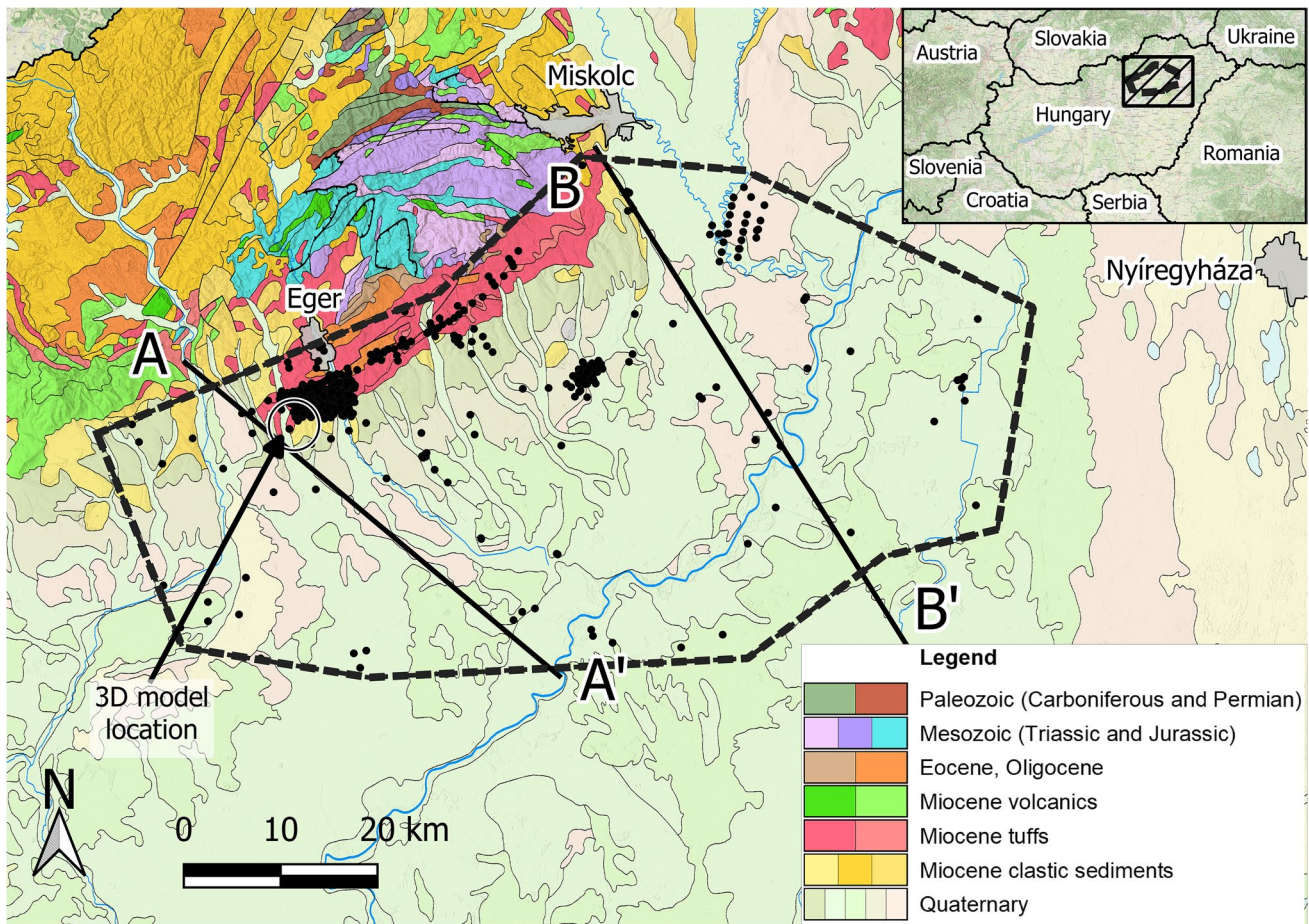


Fig. 1 Geographical location and geological map of northeast Hungary (MBFSZ 2017). The area delimited by the dashed black line shows the selected test site, black dots represent the nonequidistantly distributed investigated wells. The circle indicates the 3D modelled

location site (see section ‘Results’). Profile AA’ and BB’ show the 2D cross-section lines of the predicted specific geothermal energy (section ‘Discussion’)

database of these wells contains detailed descriptions (e.g., geological profiles, cover and filtration, screen position, flow rate and water level). The Cadaster of Hungarian Thermal Water Wells is a kind of book series edited by the former Hungarian Mining and Geological Survey (MBFSZ). (From 2022, the Institute falls under the Supervisory Authority for Organized Activities.) It possesses important details of every thermal water well drilled in Hungary, with certain volumes being supplemented by well logging datasets.

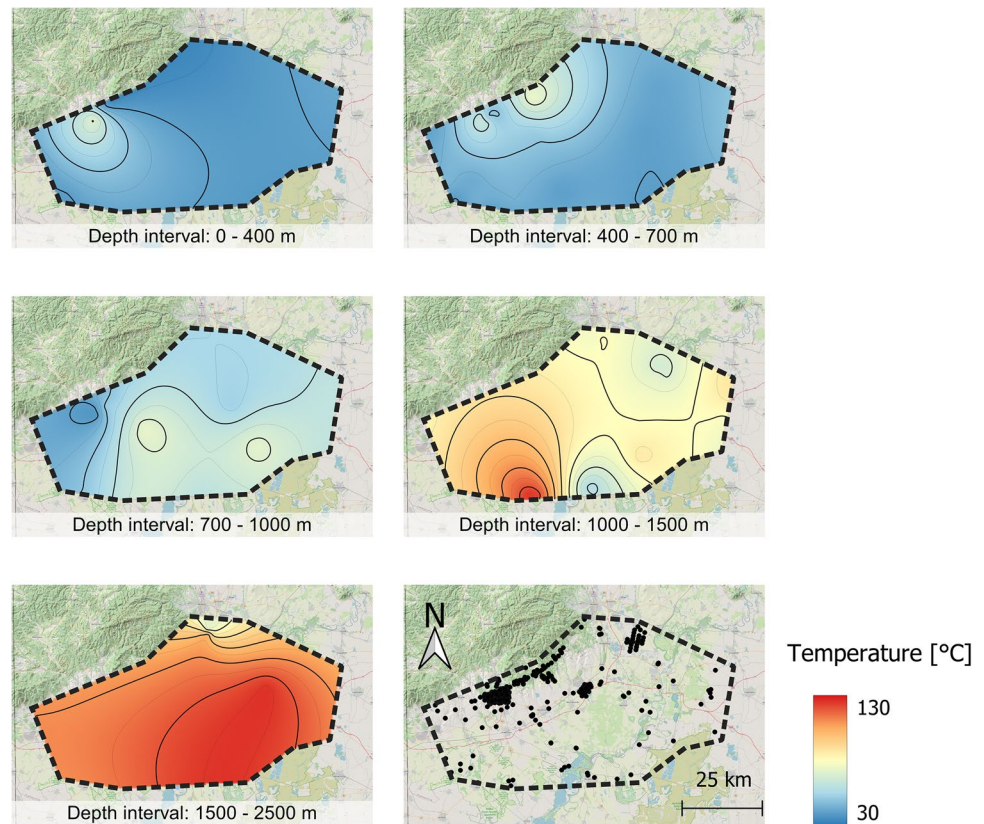
A requirement of the created database is that it includes every useful piece of data about the structure and condition of the well, the geological environment, the hydrogeological properties, technical parameters, testing results and temperature regimes. The database includes highly detailed data for the selected test area in northeast Hungary. The delineation of the investigated area was based on geologic considerations connected to former petroleum explorations and on existing analysis of demands on geothermal energy. The methodology that was developed as part of the study in this area may be applicable to the investigation

of other areas. After the first stage of database building, the already available information was used for a detailed geothermal characterization of the area of interest. A map of the depth and thickness of the geological formations has been created. The most important results are the temperature distribution maps for different depths and different geologic units; an example corresponding to the investigated area is presented in Fig. 2. Different researchers worked with different algorithms to generate different resolutions (Békési et al. 2017; Dövényi et al. 1983) and this study obtained similar temperature distributions in similar depth ranges. By increasing the depth or distance from the karstic bodies of Bükk Mountains, the temperature becomes higher.

Web-based data management

A geoinformation system has been developed for managing the scanned documents of the investigated wells. The achievement of the main objectives required the collection and analysis of a large dataset. The sources of the most

Fig. 2 Temperature distribution maps for different depth intervals at the investigated area, Bükk Mountains, northeast Hungary



important data were the documentation of numerous wells drilled over the investigated test area during the last 70 years. Each of these wells has its own folder, which includes all the documents generated in relation to the well during its lifetime. The folders of the wells, in their paper-based formats, are stored and managed by the national data repository of Hungary. In fact, scans of the necessary documents in the appropriate folders were purchased for the study. In order to facilitate browsing and searching functions, a web-based system centered on the documents was designed.

The most important information contained in those documents that typically appear on the web pages of the investigated wells (and their number) includes the following:

- Geological and technical plans of the wells (130 documents)
- Daily geological and drilling reports (1,637 documents)
- Plans of drill stem tests (86 documents)
- Reports on the results of drill stem tests (435 documents)
- Reports on the analysis of fluid samples (87 documents)
- Scanned open-hole wireline logs (1,009 documents)
- Final report on the different operations, e.g., drilling, coring, well logging, casing, testing (76 documents)
- Other documents and web links (1,075 documents)

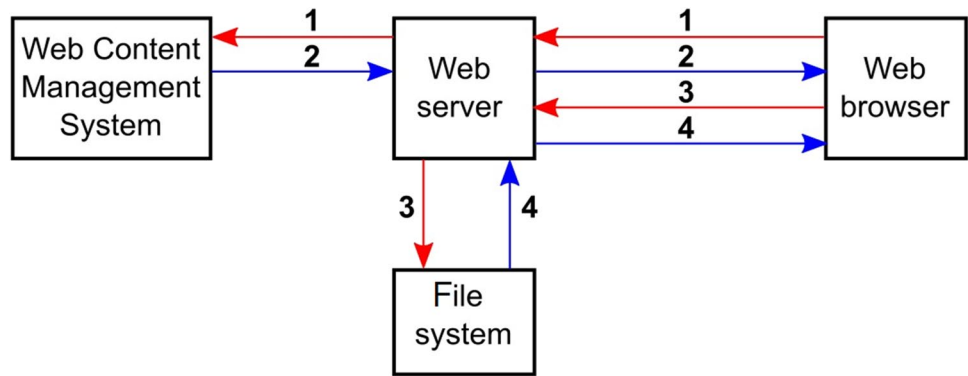
The schematic structure of the developed geoinformation system is shown in Fig. 3.

Geothermal potential estimation method

The overall cost of high-resolution geological exploration is generally high (Turai-Vurom 2013). In many cases, however, the cost and time requirements of the required geological exploration cannot be estimated easily. It is also difficult, for the purposes of the potential investors, to numerically express the geothermal potential of an investigated area. In this paper, a quick evaluation method is presented using only existing infrastructure and geological information to provide relevant information for potential investors.

To assess the potential use of the investigated wells for geothermal energy production, an innovative and easy-to-use experimental method is described in the following. The multiple evaluation methods are applicable to estimate the geothermal energy potential for a certain well. For each well, the most important evaluation parameter is weighted by 1–5 points (1 point = weak, 5 points = excellent). Based on the obtained values, the potential for the use of an investigated area for geothermal energy production can be divided into three groups:

Fig. 3 The schematic structure and working principle of the developed geoinformation system. Legend: (1) request for an HTML page (which displays the list of documents belonging to a well), (2) sending the HTML page, (3) request for a file (a scanned document selected from the list of documents), (4) sending the required file



- Evaluation result <3.0 (geothermal use is not recommended)
- 3.0 ≤ evaluation result <4.0 (geothermal use is recommended)
- 4.0 ≤ evaluation result ≤ 5.0 (geothermal use is strongly recommended)

Consider an example involving well DEP-37 (Demjén Pentecostal) in the investigated area. The names of the eight different studied geological and infrastructure parameters in the proposed evaluation system and the qualification of the well are indicated in Table 1. The main score can be first approximated by the mean of the individual points. However, this approach gives equal weight to each of the points. To give a more robust estimate, the use of the most frequent value (MFV) method is recommended, which calculates the weighted average of the evaluation points in a statistically highly efficient algorithm (Steiner 1988, 1991; Szűcs et al.

2006; Szabó et al. 2018). The MFV is calculated from the following implicit formula:

$$MFV = \frac{\sum_{i=1}^n x_i \frac{\epsilon^2}{\epsilon^2 + (x_i - MFV)^2}}{\sum_{i=1}^n \frac{\epsilon^2}{\epsilon^2 + (x_i - MFV)^2}} \tag{1}$$

where x_i is the i -th evaluation value, ϵ is called a dihesion and it represents the scale parameter of the Cauchy-type weight function $\epsilon^2 / [\epsilon^2 + (x - MFV)^2]$. If one cannot decide the relative importance of the individual scores, the MFV algorithm weights them automatically in an iterative process to give an optimal solution. The value of MFV is estimated in a recursive algorithm as it is found on both sides of Eq. (1), meanwhile the dihesion is also automatically updated. The advantage of the aforementioned method is that the MFV is found independently of the statistical distribution

Table 1 The proposed evaluation method applied to well DEP-37, Bükk Mountains, northeast Hungary

| Parameter No. | Evaluation parameter | Scale | Value | Point (x) |
|---------------|--|--|-----------------------------|-----------|
| 1 | Year of drilling | (1) 1970, (2) 1971–1980, (3) 1981–1990, (4) 1991–2000, (5) >2000 | 1986 | 3 |
| 2 | Well function | (1) technically eliminated, recultivated, (2) technically eliminated, (3) secured with cement plug, (4) designed for oil production, (5) water production, water repellent, gas production | Designed for oil production | 4 |
| 3 | Fluid volume [m ³ /day] | (1) 1–20 (2) 21–40, (3) 41–100, (4) 101–500, (5) >500 | 87.7 | 3 |
| 4 | Average fluid temperature [°C] | (1) 4–20, (2) 21–40, (3) 41–70, (4) 71–100, (5) >100 | 33.8 | 2 |
| 5 | Geothermal energy [MJ/d] from the pore-fluid | (1) 0–0.5, (2) 0.5–1, (3) 1–5, (4) 5–10, (5) >10 | 12.3 | 5 |
| 6 | Maximum specific (average) geothermal energy (MJ) that can be extracted from the 1-m environment of the well | (1) 0–100; (2) 101–200; (3) 201–400; (4) 401–800, (5) >800 | 321.1 | 3 |
| 7 | Total length of screen section [m] | (1) 1–20, (2) 21–40, (3) 41–70, (4) 71–100, (5) >100 | 16.5 | 3 |
| 8 | Total distance of infrastructure [km] ^a | (5) 0–5, (4) 5–10, (3) 10–20, (2) 20–30, (1) >30 | 4.26 | 5 |
| | | | | MFV = 3.0 |

^aTotal distance of infrastructure is the sum of distances from the closest public road, electric grid and the closest settlement

of input data (e.g., for non-Gaussian distributed data or in the presence of outliers). By applying Eq. (1), the robust algorithm runs over 15 iterations and gives $MFV = 3.00$ and $\varepsilon = 3 \cdot 10^{-3}$. On the spider chart in Fig. 4, besides the serial number and value of the specific parameters, the MFV of the parameters is shown with a dashed line and also with a number in the middle supporting the simple interpretation process. However, the general geothermal parameters are relatively good, but the present technical condition of the investigated well is quite poor. As a result, the geothermal use of the given well is to be considered.

Basin modelling

Integrated basin and petroleum system modelling are used to understand and reconstruct the geological and thermal evolution of a sedimentary basin, using mathematical approaches to derive the history of generation, migration, and accumulation of petroleum (Ungerer et al. 1990). Doing so, porosity, permeability and thermal properties of the basin are modeled (Hantschel and Kauerauf 2009). In the case of missing data or data that are old, suspect or undetermined, the integrated basin modelling method might be a tool to predict necessary information for geothermal resource assessment (Nelskamp and Verweij 2013). In the absence of seismic information, and other basic petrophysical values or fault databases, a one-dimensional (1D) basin modelling approach was first applied to the formerly defined 20 sediment layers as thermal units, well by well, during which

stress and heat flow vectors were assumed to be horizontal. From these results, a 3D approximate model of the investigated Eger-Demjén region was created. Supposing that the investigated layers are roughly subhorizontal, instead of a real 3D kriging method, a 2.5D horizontally biased kriging algorithm was applied (Nash et al. 1988).

In the truncated workflow of the integrated basin and petroleum system modelling, the assignment of geological events, such as sedimentation, erosion and hiatus, was the first step, followed by the pressure and compaction calculation. In this phase, as new sedimentary layers started covering the formerly settled ones, because of the weight of the subsequent sedimentary material, porosity decrease was calculated by a compaction law (Hantschel and Kauerauf 2009) based on the widely used Terzaghi's effective stress definition (Osipov 2015)

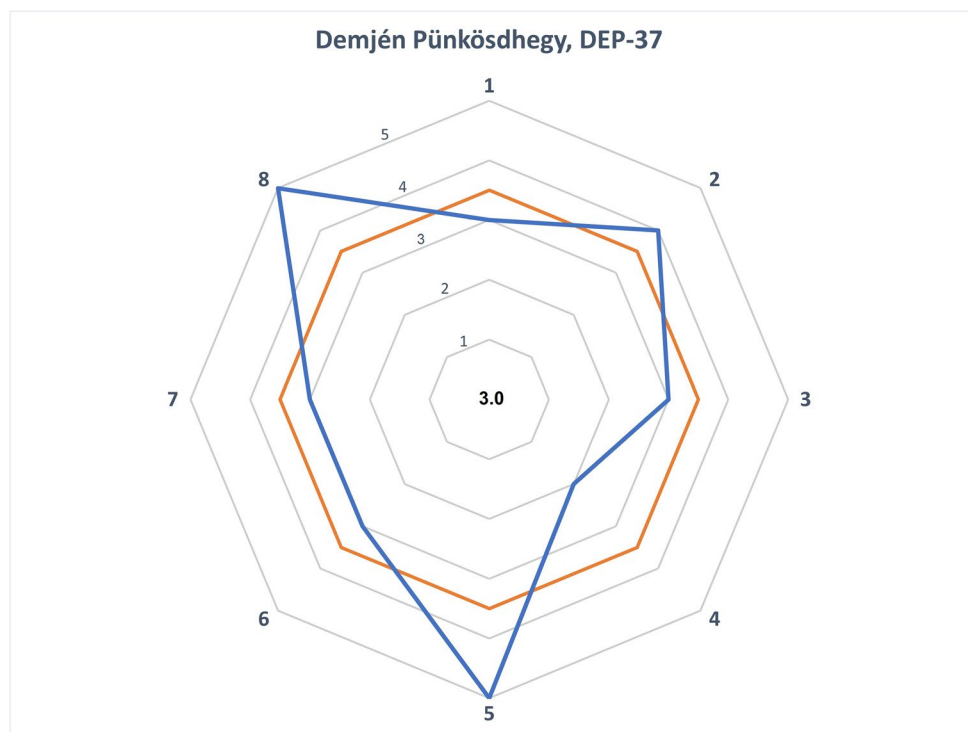
$$\frac{\partial \phi}{\partial t} = -C_T \frac{\partial \sigma'_z}{\partial t} \quad (2)$$

and

$$\sigma'_z = p_1 - p \quad (3)$$

where ϕ is the porosity (between 0 and 1) of a given sedimentary layer, t is time (My) from the beginning of the sedimentation process, C_T is Terzaghi's compressibility factor, which is decreasing during compaction, σ'_z is the vertical component of the effective stress (MPa), p_1 is the load pressure of the overburden sediment (MPa), p is pore pressure

Fig. 4 Distribution of the parameters examined for geothermal potential evaluation in well DEP-37, Bükk Mountains, northeast Hungary. The most frequent value of the parameters is indicated in the middle. Axes are defined according to parameter numbers in Table 1



(MPa). The third crucial phase was heat flow analyses, in the pursuance of which one must build up a crustal model to calculate the amount of heat flowing into the sediments; then one must calculate the temperature in the sediment body, layer after layer. It is a thermal boundary value problem

$$q = \lambda_b \frac{T_b - T_{swi}}{h_1} \quad (4)$$

where q is heat flow (mW/m^2) between two boundary layers with different temperatures, λ_b is the bulk thermal conductivity of the layers (W/mK), T_b is the base lithosphere temperature (m), T_{swi} is the sediment–water interface (SWI) temperature (K), h_1 is the thickness of the lithosphere (m) (Hantschel and Kauerauf 2009). In Eq. (5), indices m, c and s refer to the mantle, crust and sediment part of the thicknesses (m) and thermal conductivities (W/mK), which can be used to express

$$\frac{h_1}{\lambda_b} = \frac{h_m}{\lambda_m} + \frac{h_c}{\lambda_c} + \frac{h_s}{\lambda_s} \quad (5)$$

During the computational process, the heat flow equation was applied layer by layer in the sequence of the subsequent geologic layer creation processes. The heat flow from the base or from the formerly settled layer boundary was not constant because of the differences in radioactive element content (Rybach 1973)

$$Q_r = 0.01\rho_r(9.52U + 256\text{Th} + 3.48\text{K}) \quad (6)$$

where Q_r is the radioactivity produced heat flow ($\mu\text{W/m}^3$), ρ_r is the rock density (kg/m^3), and U, Th and K are the concentrations of uranium (ppm), thorium (ppm), and potassium (%) of the layers, respectively. Pore fluids do not generate radioactive heat; this way the increase of vertical heat flow (Δq) is

$$\Delta q = (1 - \phi)hQ_r \quad (7)$$

where h is the thickness of the layer (m). The basin evolution has a time dimension. Deposition and erosion events, and basal and SWI temperature changes cause transient states. The nonsteady 1D temperature distribution along a vertically directed coordinate axis z can be described by the following differential equation (Hantschel and Kauerauf 2009)

$$\rho c \frac{\partial T}{\partial t} - \frac{\partial}{\partial t} - \left(\lambda \frac{\partial T}{\partial z} \right) \quad (8)$$

where c and ρ are bulk heat capacity (J/kgK) and density (kg/m^3), T is the temperature of the sediment (K), t is the time. As sedimentary layers deposit through time, their weight starts to press the lithospheric slab into the hot asthenosphere. Following this process via the Airy model (Allen and Allen 2013), sinking and heating of the basement and

the subsequent layers were taken into account. Determining the aforementioned values from the beginning of the deposition of the sediments (with different sedimentation rates), layer by layer, following the erosion events as well, a dynamic model was achieved. At some sites, multiple-borehole temperature measurements from successive logging runs were available. For heat calibration of these 1D models, the Horner plot correction procedure was used (Deming 1989).

Results

1D basin modelling

From the sometimes overly sophisticated or overly simplified drill-hole reports, 20 identifiable layers could be extracted from more than 1 km length. These layers were defined as well-defined paleoenvironmental units. For one drill hole, these (maximum 20) layers were modelled. The thermal history of every well was included and the present-day heat distribution was generated by the 1D basin modelling algorithm. To identify the geological layers as modellable thermal units, a heterogeneous and incomplete dataset of 161 boreholes was used. First, the geologic ages in the form of million years had to be assigned to the layers. The ages of the lithofacies from the Paleogene and lower Miocene were documented in the Encyclopedia of Pannonia (Arcanum 2019). Other geologic ages were generally used according to the International Chronostratigraphic Chart (Cohen et al. 2013). Then there was the assumption that the Miocene erosion had taken place, which extended from 11.6 to 12.6 million years (Vrsaljko et al. 2006). During that epoch, the studied region was an archipelago, and in some places, the area was seriously denuded, while not in others. The possible eroded sediment thicknesses were generated well to well, assuming a continuous sedimentation speed. Since the rate of Miocene erosion was not known, a similar rate was assumed as if the settlement happened (Elias and Mock 2013). The changing water depth in the sedimentary basin (paleo water depth, PWD), the temperature of the interface between the upper surface of the sediment and the covering waterbody (sediment–water interface temperature, SWIT), then the changing of the heat flow in the basin throughout the investigated layer-generating time (heat flow history), had to be set. The estimation of the PWD was made based on literature data (Sztrákó 1973), which was limited by uncertainties in space, like seriously changing borders of the shorelines and sometimes deep or shallow water depth changes over time. The PWD data in a semiquantitative form were determined by foraminiferal facies of the investigated region (Sztrákó 1973), which was used to reconstruct the paleowater depth oscillation (Fig. 5).

In the Eger-Demjén region, during the modelled time range, transgressions and regressions of the sea followed each other, sometimes with erosion stages. Step by step, this sea environment becomes shallower in time, later transforming into a freshwater-filled basin. At the end, during the Eggenburgian, continental facies become prevalent. The interface temperature of the upper sedimentary layer under the waterbody of the sediment gathering basin (SWIT) is an upper limit in the definite integral counting of the heat spreading processes in the heterogeneously layered basin fill. The position of this surface is changing through time. Knowing that the investigated area (Eger-Demjén region, north-east Hungary) today can be found in the Northern European region on the latitude of 51st degree, applying a general sea surface temperature model (Wygrala 1989), the global mean surface temperatures at sea level today and in the past can be determined, considering the global historic climate changes and the continent wandering events. From that data and the water-depth changing scenario, the SWIT values through the investigated geologic period were estimated (Table 2).

From the Eocene up to Oligocene, oceanic-environment-generated sediments were disrupted completely by strong erosion events (Keveiné Bárány 1992). Because of this, the last well-documented and modellable 40-mW/m² heat flow value was applied. The construction of the multiple-rifting scenario of the Pannonian Basin is a complex problem. Thermal history data were taken into account by the application of burial and tectonic history of the Pannonian Basin. It is a five-step model, created and continuously developed by several authors (e.g. Royden et al. 1983; Lenkey et al. 2002; Gyollai 2007; Horváth 2007; Dövényi 2016; Blahó 2011; and, just for the given area from the viewpoint of the tectonic phases, Petrik et al. 2016). The model developed applies the McKenzie method (McKenzie 1978) using only one pulling type of rifting event; however, it was necessary to create the five-step scenario as a composite but realistic method. Additional necessary factors, like stretching of the crust and mantle, were taken into account in the article of Huismans et al. (2001). The possible heat-flow history, applying the

previously mentioned literature data, can be seen in Fig. 6 (Royden et al. 1983; Huismans et al. 2001; Gyollai 2007; Horváth 2007; Blahó 2011; Dövényi 2016; Petrik et al. 2016). In the first stage, from about 27 up to 20–21 million years, a north–south and a northwest–southeast-directed crust thickening was characteristic. During the second stage, from approximately 20–21 to 12 million years, there was the first rifting phase or first extension event, affecting the central part and the borders of the basin. The third phase is a short inversion period from 12 to 9.5 million years, with identifiable erosion surfaces and a hiatus in the basin fill. The border of the synrift–postrift phase was signaled by arching or missing Sarmatian sediments, or sometimes the thinning of Badenian–lower Pannonian layers (Horváth 2007). During the fourth phase, from the beginning of the Pannonian stage, the central part of the basin was sinking. At that time, the stretching of the mantle was more significant than the thinning of the crust. This second extension or rift phase (from 9.5 to 5.5 million years) was the result of the former arching of the asthenosphere. The last step, starting about 4 million years ago, was the inversion of the Carpathian Basin, which has lasted to the present time.

Table 2 Boundary condition adjustment for the simulation of the basin creation and filling up history

| Age [million years] | Paleowater depth [m] | Sediment–water interface temperature [K] |
|---------------------|----------------------|--|
| 0.00 | 0 | 10.00 |
| 5.33 | 0 | 12.59 |
| 11.60 | 0 | 16.07 |
| 12.60 | 0 | 17.35 |
| 27.82 | 180 | 18.20 |
| 30.10 | 100 | 19.44 |
| 31.37 | 100 | 19.58 |
| 33.22 | 60 | 19.79 |
| 33.90 | 40 | 20.87 |

Fig. 5 Oscillation of the sea level in the surroundings of Demjén during the Paleogene age (re-edited after Sztrákos 1973)

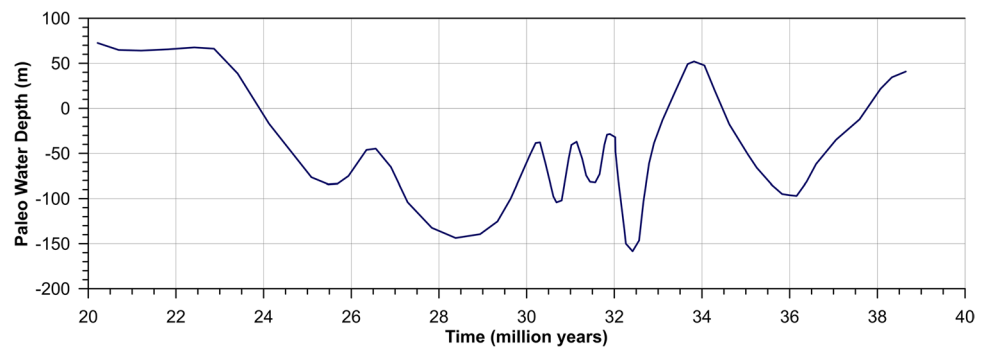
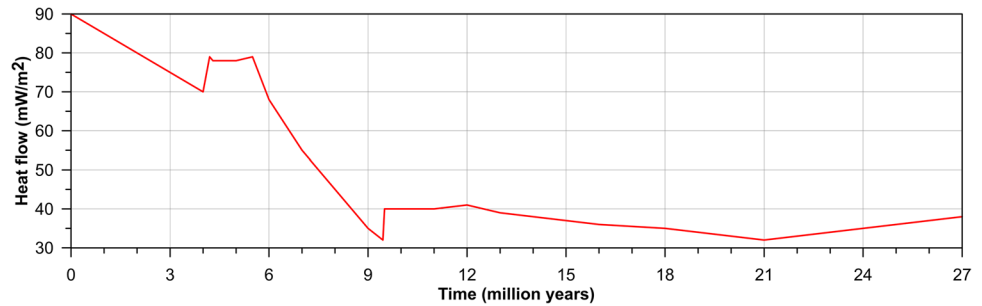


Fig. 6 Possible heat flow trend of the Pannonian Basin from 27 million years to the present day, a literature-based review



For the simulation performed here, an iterative finite element algorithm was used, where the maximum cell thickness was 1 m thinner than any modelled unit. The time step duration was 0.1 million years, because every modelled geological phenomenon lasted longer than this period. Depth-related temperature, bulk density and heat capacity curves were generated, together with an overlay showing the vertical thermal conductivity as a color scale in the background

(Fig. 7). Porosity was estimated as well, both in time and depth for later computational steps. Using a 283.15 K surficial reference temperature (T_r), the amount of heat stored in unit volume of the drill-hole surrounding rock was determined for the whole drill-hole by the following equation:

$$Q_{st} = \sum_{i=1}^n c_i (T_i - T_r) \tag{9}$$

Fig. 7 Result of the 1D basin modelling process in well Demjén-Püspökhegy 33, Bükk Mountains, northeast Hungary

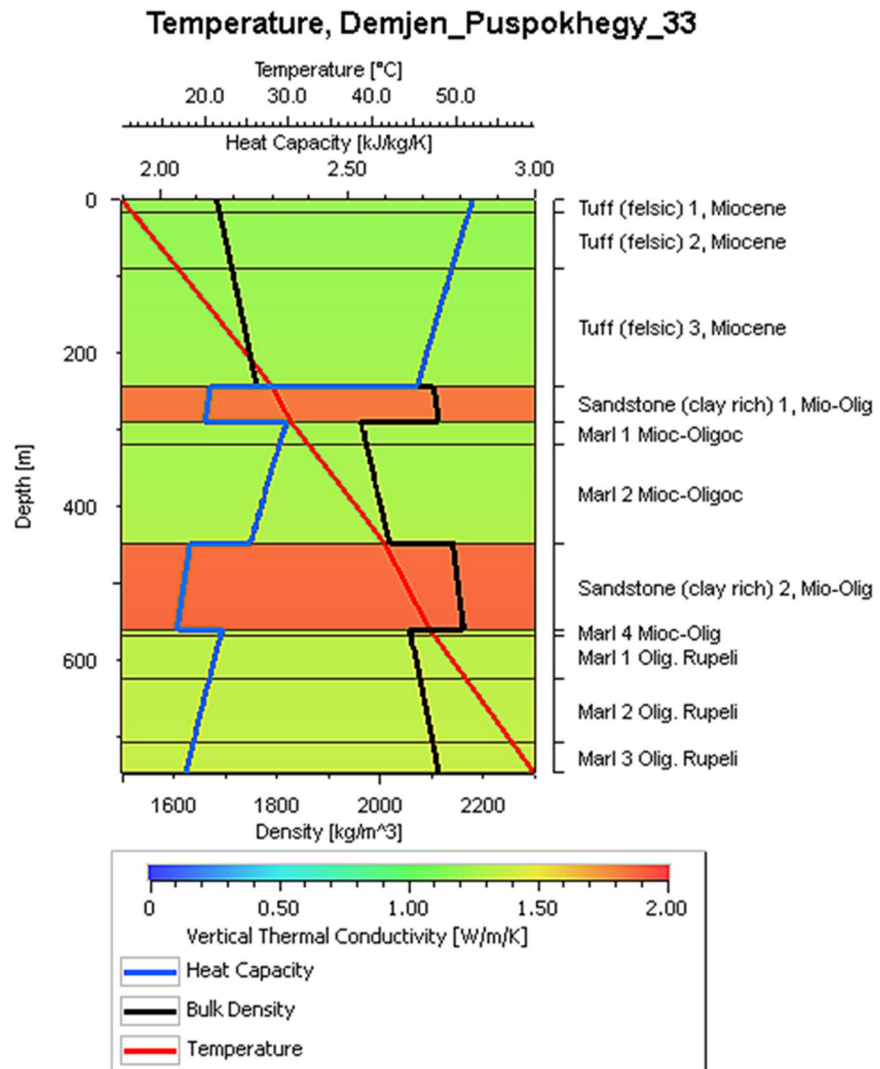
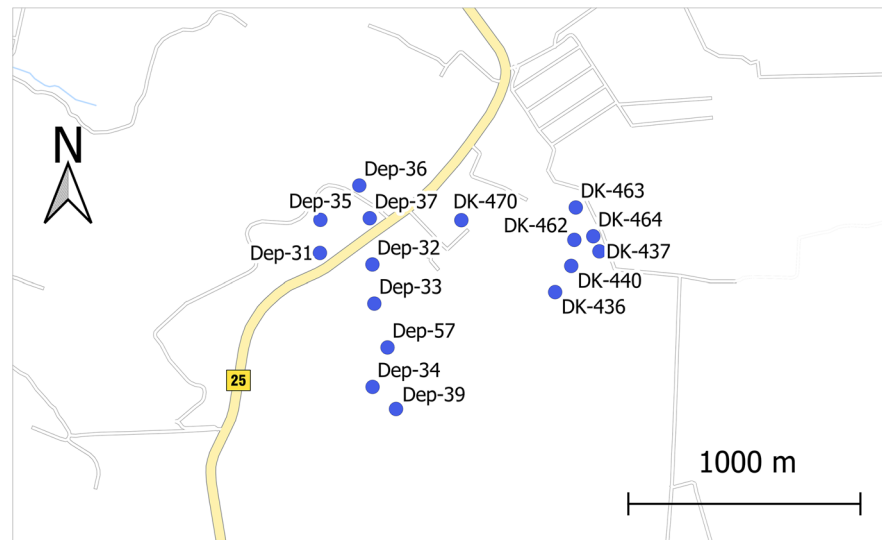


Fig. 8 The nine drill holes selected for investigation from the research area of Demjén-Püspök Hill (Dep-) and seven boreholes from the area of Demjén South (DK-), Bükk Mountains, northeast Hungary. The yellow line is a road



where Q_{st} is the stored amount of heat in a whole drill-hole (J), c_i and T_i are heat capacity (J/kgK) and temperature of a given 1-m-thick layer element (K), respectively. As one can see from Fig. 7, the temperature distribution of this dynamic model changes by depth, showing that a heat flow analysis that is based on a constant thermal gradient would be an unpunctuated approximation.

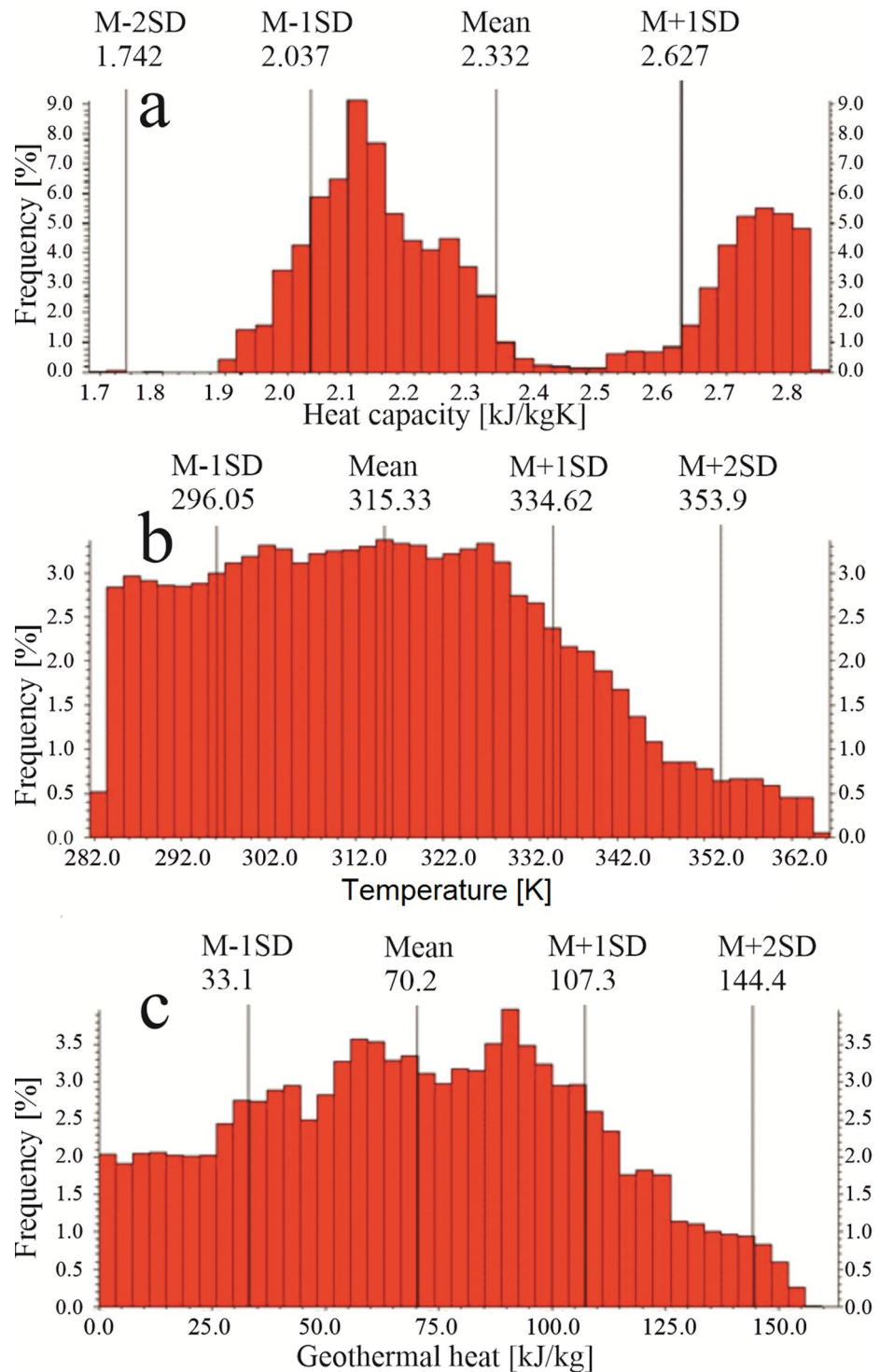
3D stratigraphic/petrophysical modelling

To extend the validity of the constructed 1D models, a 3D sample unit was created from 16 drill holes (Fig. 8). Sixteen neighboring drill holes were chosen with almost similar depth ranges (700–1,200 m) and in close proximity. The modelled spatial body had 1,210-m range in the geodetic X direction, 970 m in the Y direction and 1,225 m in the Z (vertical) direction. The applied spacings were chosen as 10 m in the horizontal directions and 5 m vertically. The 20 dominant layers, which were the basic units in the basin modelling process, were used as stratigraphic units and the data of the formerly created 1D basin models (like heat capacity and temperature distribution together with the accounted geothermal heat values as point data) were applied as input for the 3D modelling. The superficial reference temperature for the temperature correction was 283.15 K as an average annual temperature for Hungary. Generated temperature values at every meter of the drill holes' depth were reduced by the reference temperature. Corrected temperatures were multiplied by heat capacity values of the given 1-m-thick slice of the layers, generating geothermal heat amount, and considered true in a 1-m-thick volume unit around the given drill hole. The layer structure

of the 16 drill holes followed two well-defined series. Drill holes on the western side (Dep-31, Dep-32, Dep-33, Dep-34, Dep-35, Dep-36, Dep-37, Dep-39, Dep-57) contained almost every layer from the general layer structure of the area in almost the same thicknesses. On the other hand, layers on the east side of the sample area (DK-436, DK-437, DK-440, DK-462, DK-463, DK-464, DK-470) started basically with tuffs, ending with marls.

Since the spatial distribution of the boreholes is rather uneven, showing mostly a northeast–southwest-directional clustering on the northern and southern sides of the sample area, a robust and spatially governable spatial interpolation method was necessary for the modelling. Among others, the two generally applied algorithms are the inverse distance weighting and ordinary kriging (Afzal 2018; Yi-Hwa and Ming-Chin 2016). The two methods are similar to each other, in the sense that both of them are counting the identifiable parameter in the voxel midpoint from the nearest known values in a given adjustable environment, applying a moving weighted average with different weight values. Departing from the known values, the weights become smaller (Babak and Deutsch 2008). The weighting can be deterministic (inverse distance weighting, IDW) or statistical (e.g., kriging and its modifications). The advantage of deterministic methods is their robustness, but they are sensitive to the number of used points and the value of the exponent. By applying weighting, spatial directions can be followed more sensitively. Since spatial arrangement of the drill holes is uneven and directed, and the used amount of data is limited (only 16 drill holes were used for creating the 3D models), it was expedient to apply a mathematically exact method in which spatial directivity could be well managed. For that purpose, ordinary kriging seemed to be the more advantageous

Fig. 9 Histograms of modelled **a** heat capacity, **b** temperature and **c** geothermal heat in the 16 boreholes, Bükk Mountains, northeast Hungary



one. Another difficulty was the statistical behavior of the input datasets (represented in Figs. 1–2). Because the sample area was possibly divided into pieces by faults, but the fault database was not available, the applied interpolation algorithm had to handle different data populations. On top

of that, the modelled physical parameters showed different statistical distributions (Fig. 9). The histogram of the heat capacity (Fig. 9a) shows two well-defined bell-shaped data populations. A more uniform distribution can be seen on the histogram of the modelled temperature data (Fig. 9b).

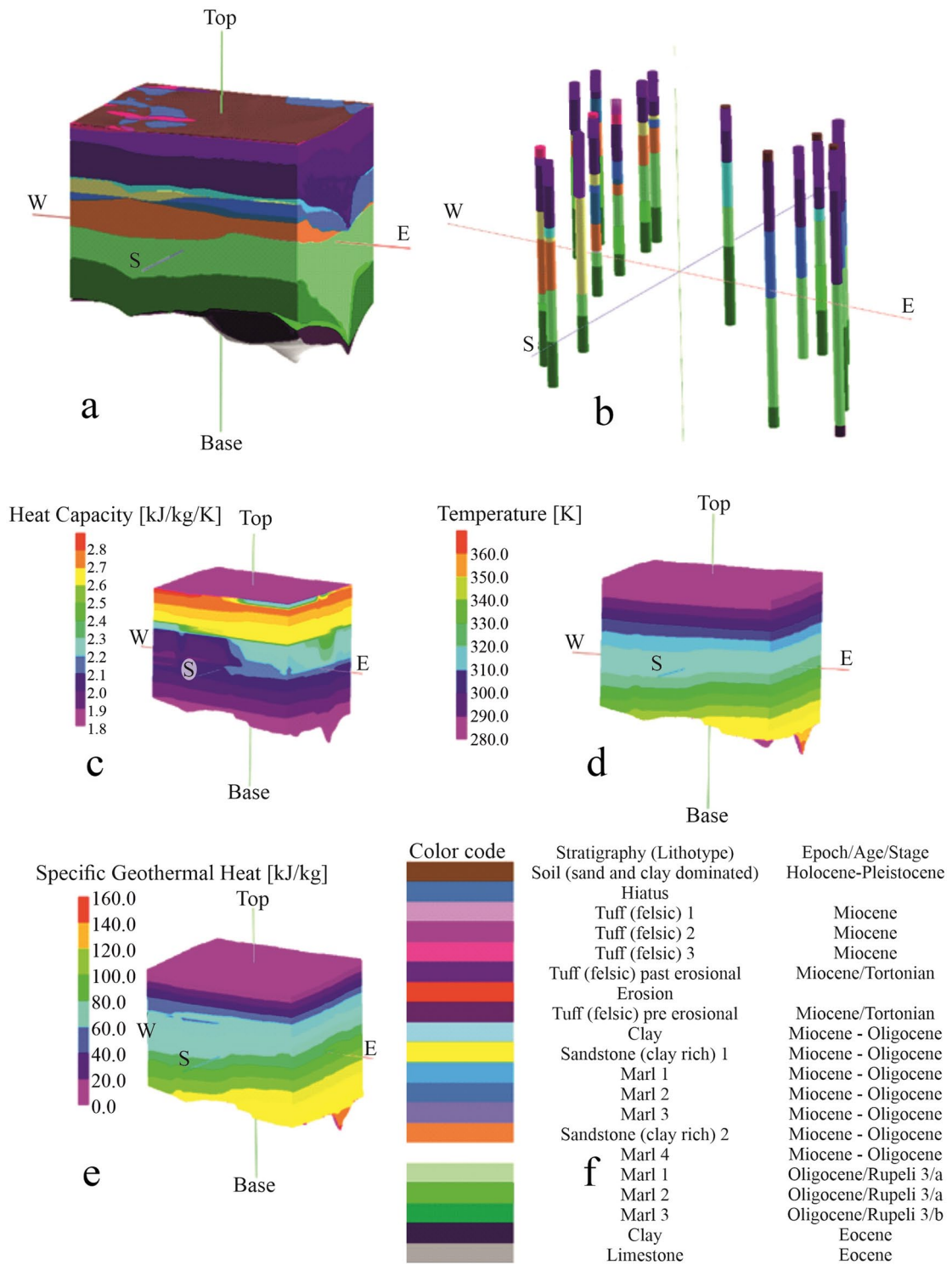


Fig. 10 **a** Stratigraphic model of the studied site. **b** Locations of drill holes with stratigraphic units involved in the calculations. **c** Modelled heat capacity layering. **d** Modelled temperature distribution. **e** Modelled geothermal heat structure. **f** The stratigraphic units of the sample area and their color codes, used in both the basin and structural modelling, involving the 20 dominant layers that were the basic units in the basin modelling process

The tilted and skewed dataset might also be the result of two data populations. Since the geothermal heat amount is the heat capacity multiplied by the temperature, the dataset in Fig. 9c shows the mixed behavior of the previous two datasets.

Applying an ordinary kriging algorithm, the structural connection between the layers was approximated by the drill-hole locations and the directions of the similar layer structures. It can be seen in Fig. 10 that because of

Table 3 Bottom-hole temperatures (from the drillers’ rotary table): noted bottom-hole static temperature by the Horner method, modelled temperature at the given (deepest modellable) depth using the finite element method in basin modelling, and the difference between the basin-modelling-derived temperature and the Horner-corrected bottom-hole temperature

| Drill-hole | Bottom-hole depth [m] | Static temperature [°C] | Modelled temperature/depth [°C/m] | Temperature difference [°C] |
|------------|-----------------------|-------------------------|-----------------------------------|-----------------------------|
| Dep-31 | 720 | 56.6 | 62.5/716 | 4.2 |
| Dep-32 | 720 | 56.6 | 60.8/715 | 1.7 |
| Dep-33 | 750 | 57.7 | 59.4/747 | 2.3 |
| Dep-34 | 900 | 62.7 | 65.1/896 | 0.6 |
| Dep-35 | 706 | 56.1 | 56.6/704 | −0.01 |
| Dep-36 | 700 | 55.9 | 55.8/698 | −0.7 |
| Dep-37 | 700 | 55.9 | 55.3/698 | 6.3 |
| Dep-39 | 930 | 63.7 | 70.0/927 | 10.3 |
| Dep-57 | 900 | 62.7 | 73.0/897 | 16.8 |
| DK-436 | 1136 | 69.9 | 86.7/1136 | 19.6 |
| DK-437 | 1200 | 71.6 | 91.2/1196 | 9.0 |
| DK-440 | 875 | 61.9 | 71.0/870 | 10.1 |
| DK-462 | 900 | 62.8 | 72.9/898 | 13.1 |
| DK-463 | 1000 | 65.9 | 79.0/995 | 18.2 |
| DK-464 | 1125 | 68.8 | 87.0/1122 | 4.8 |
| DK-470 | 900 | 62.7 | 67.4/892 | 5.9 |

the similar northeast–southwest direction on both sides of the 3D modelled sample area, in the case of stratigraphic modelling, the long axis of the ellipse from the kriging was adjusted in parallel to this general structural direction. Thus, on the semivariogram, using a locally well-approximating linear distribution model without a nugget effect, the Pearson’s correlation coefficient was high enough (0.82). The heat capacity, temperature, and specific geothermal heat datasets needed another variogram adjustment. In the case of the physical parameters, based on the 1D basin model, a Gaussian distribution with a nugget effect produced favorable starting correlation values. Because of the strong effect of the structural directions, an inverse distance weighting algorithm would not be so effective. Between the western and eastern side, existence of a fault parallel to the northeast–southwest directions of the drill holes and structures, might be assumed. The resultant 3D stratigraphic and petrophysical models can be found in Fig. 10.

Bottom-hole temperature data of the disturbed formations, gathered by well logging operations, were used for the Horner method (Timko and Fertl 1972) to create bottom-hole static temperature or initial formation temperatures (Table 3). The table also contains the basin modelling approach’s modelled temperatures. Because the temperature modelling in the basin modelling approximation is created by a finite element mesh, the lowest countable points in this net were in the 2–8 m higher position than the real true depths of the holes. It is concluded that, with increasing depth (Fig. 11), the temperature differences between the two modelling considerations become more expressive.

Discussion

In the geothermal reuse of an abandoned hydrocarbon well, it is essential to determine the amount of energy stored in the well environment as accurately as possible. The available geothermal energy is a very important factor in the proposed

Fig. 11 Differences in the temperatures between the values obtained by the Horner method (measured) and the basin modelling approach, as a function of total depth of borehole

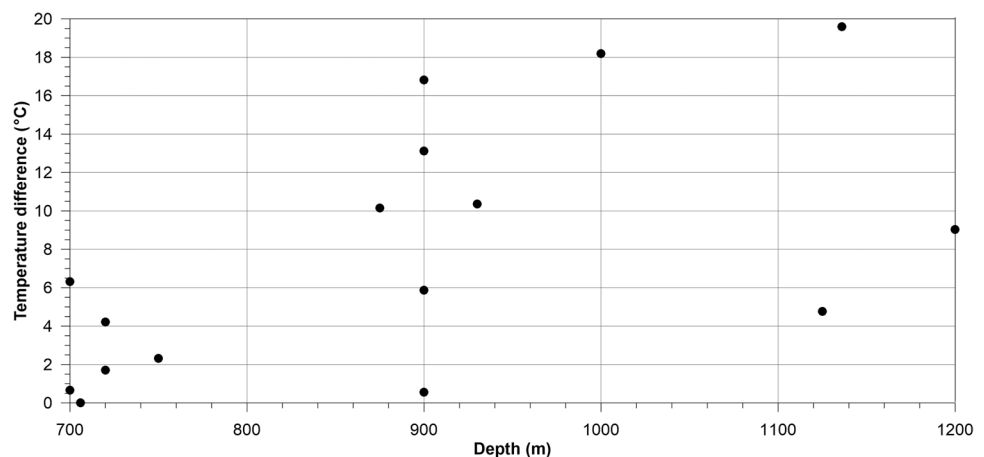
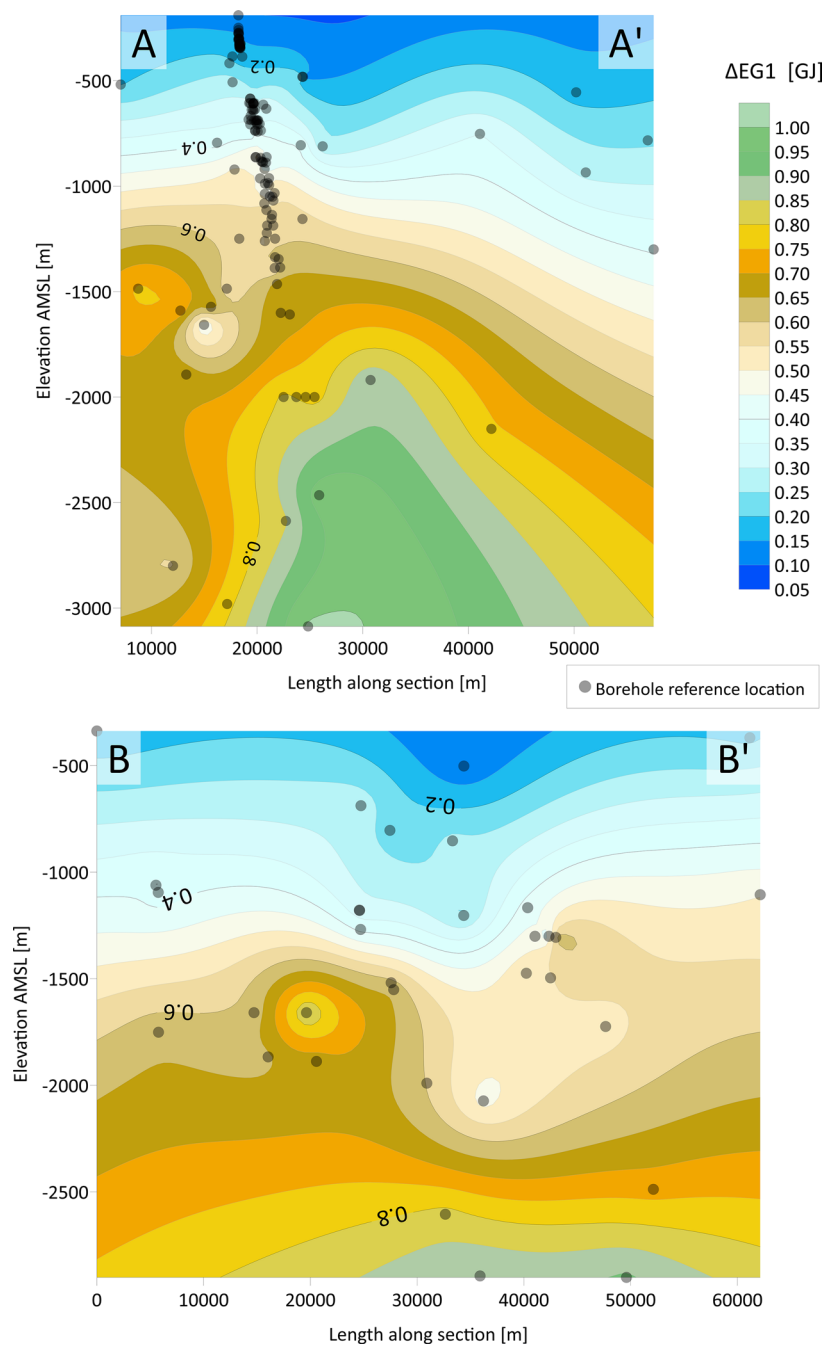


Fig. 12 2D cross-sections of the predicted specific geothermal energy (EG) in the research area, Bükk Mountains, north-east Hungary: **a** section A–A', **b** section B–B' (see Fig 1)



assessment workflow. Each well, drilled for a different purpose (fluid mining, solid minerals mining, geological exploration, construction geology-geotechnical, geothermal, etc.), has a definable geothermal energy potential. This study has also developed an analytical method to determine the maximum amount of energy (rock and fluid) stored in the well surroundings. To develop a well-applicable method, the Gazo method (Gazo 1992) to determine the maximum amount of geothermal energy that can be extracted from an arbitrary volume was used. Gazo's method was applied by Barylo (2000) to estimate the geothermal energy of an

area in Ukraine; however, Gazo's method yields an approximation, as it uses average parameters of the given volume (average porosity, average temperature, average rock density, average fluid density, and average specific heat values), which makes the determination of energy rather inaccurate for large volumes.

More accurate calculation of the geothermal energy content in the vicinity of a given well requires the determination of the detailed spatial distribution of physical and thermal parameters and the spatial integration of the amount of differential energy. The distribution of the parameters needed

Table 4 The characteristics of 20 wells with the smallest and 20 wells with the largest specific energy content, in the investigated area, Bükk Mountains, northeast Hungary. For specifying the specific geothermal energy content, a volume of interest is created where the well length and radius are assumed to be 1 m, respectively. For the

total geothermal energy content, another spatial unit is determined, in which the well length is similarly 1 m, and the radius of influence is taken as 100 m. By integrating the energy contents of the units along the well length, specific and total energy values are counted. *NA* not available

| Well | Year of drilling completion | Name of settlement | Well length [m] | Specific geothermal energy content [GJ] | Total geothermal energy content [GJ] |
|--|-----------------------------|--------------------|-----------------|---|--------------------------------------|
| Wells with the smallest specific energy content | | | | | |
| DK-443 | 1984 | Egerszalók | 190 | 0.10163804 | 193112.2752 |
| K-25 | NA | Tiszakeszi | 501 | 0.107244137 | 537293.1269 |
| DK-444 | 1984 | Egerszalók | 249 | 0.133061937 | 331324.2236 |
| DK-448T | 1986 | Demjén | 300 | 0.136467199 | 409401.5974 |
| DK-441T | 1986 | Egerszalók | 260 | 0.138924067 | 361202.5744 |
| B-17 | NA | Boconád | 482 | 0.140111748 | 675338.6251 |
| De-66 | 1976 | Demjén | 272 | 0.143420081 | 390102.6195 |
| De-70 | 1987 | Demjén | 276 | 0.14531648 | 401073.4854 |
| DK-447T | 1984 | Demjén | 280 | 0.149156413 | 417637.9576 |
| DK-448 | 1984 | Demjén | 330 | 0.149556339 | 493535.9198 |
| De-69 | 1987 | Demjén | 275 | 0.150117886 | 412824.1858 |
| DK-447 | 1984 | Demjén | 305 | 0.152637023 | 465542.921 |
| DK-423 | 1979 | Demjén | 300 | 0.155109954 | 465329.8619 |
| DK-426 | 1983 | Demjén | 300 | 0.155109954 | 465329.8619 |
| K-103 | NA | Miskolc | 337 | 0.159056465 | 536020.2871 |
| DK-441 | 1984 | Egerszalók | 305 | 0.161510464 | 492606.9165 |
| De-68 | 1981 | Demjén | 386 | 0.161989086 | 625277.8726 |
| DK-442 | 1984 | Egerszalók | 308 | 0.163269354 | 502869.6093 |
| DK-450 | 1985 | Demjén | 325 | 0.164706766 | 535296.9895 |
| DK-452 | 1985 | Egerszalók | 326 | 0.164924771 | 537654.7546 |
| Wells with the largest specific energy content | | | | | |
| Verp-s-2 | 1978 | Feldebrő | 1572 | 0.684745359 | 10764197.05 |
| DK-413 | 1971 | Andornaktálya | 1601 | 0.688911656 | 11029475.61 |
| Uma-2 | 1989 | Hajdúböszörmény | 2487 | 0.729789825 | 18149872.94 |
| Verp-4 | 1979 | Feldebrő | 1590 | 0.740791421 | 11778583.59 |
| Verp-s-5 | 1979 | Domoszló | 1486 | 0.757318559 | 11253753.79 |
| El-1 | 1974 | Egerlövő | 2151 | 0.758879528 | 16323498.64 |
| Dm-4 | 1986 | Nagytálya | 2000 | 0.778351775 | 15567035.49 |
| Verp-1 | 1979 | Aldebrő | 2981 | 0.783115871 | 23344684.12 |
| Dm-3 | 1986 | Nagytálya | 2000 | 0.790092863 | 15801857.26 |
| Dm-1 | 1986 | Maklár | 2000 | 0.797883086 | 15957661.72 |
| Dm-2 | 1986 | Kerecsend | 2000 | 0.809967531 | 16199350.63 |
| HHE-T-1 | 2009 | Tiszatarján | 2604 | 0.816761075 | 21268458.39 |
| Verp-2 | 1979 | Kerecsend | 2587 | 0.842966981 | 21807555.8 |
| Hejo-1 | 1989 | Hejőpapi | 1658 | 0.854027102 | 14159769.35 |
| Szi-1 | 1972 | Szihalom | 1919 | 0.886523287 | 17012381.89 |
| HHE-JKX-T-6 | 2010 | Tiszavasvári | 2893 | 0.894305626 | 25872261.75 |
| Egyek-1 | 1988 | Egyek | 2900 | 0.908994612 | 26360843.74 |
| Ker-1 | 1964 | Kerecsend | 2465 | 0.979251377 | 24138546.45 |
| Tarna-1 | 1973 | Boconád | 3087 | 1.00783266 | 31111794.22 |
| Mn-3 | 1987 | Mezőkövesd | 1486 | 1.403831669 | 20860938.59 |

to calculate the geothermal energy potential can be well estimated using well logging methods, surface geophysical methods, and hydrogeological modelling and testing. The maximum geothermal energy contents of the surroundings of 161 wells were calculated in the research area using the proposed method. For each well, the total geothermal energy content of the 100-m-radius environment of the well and the specific (average) energy content of the 1-m-radius environment of the 1-m well length was determined. A contour map of the specific geothermal energy in the research area is shown in Fig. 12. Since the specific energy content represents the whole well (as being the average value), although this value, for the sake of the cross sections, is assigned to a single point representing the bottom of the borehole, there is likely to be a blurring of some of the detail. On the other hand, it is considered to be a convenient approach for practical applications and the overall trends are clearly visible. Based on Fig. 12, a definite growth trend in the potential of geothermal energy can be established in the north-west–southeast direction. Table 4 shows the characteristics of 20 wells with the smallest specific energy content and 20 wells with the largest specific energy content.

Conclusions

Based on a priori given data, and geologic and infrastructural considerations, a test area to investigate the geothermal potential of abandoned hydrocarbon wells has been delineated at the southern part of the Bükk Mountains, Hungary. A new, large database of many abandoned hydrocarbon wells with potential geothermal use has been built and expanded for a test site in the area. Information on geologic formations and layers, temperatures, flow rates, water chemistry as well as screening and casing, and other additional technical-related information was integrated into a joint database. The input dataset serves as the basis for the geothermal potential assessment of the selected pilot area. As a next step, a new practical and easy-to-use evaluation method has been elaborated to evaluate the abandoned wells based on eight different models and technically related parameters. Twofold analyses have been carried out, localized at a well scale and regional scale for the area, which finally may lead to further geothermal developments. The analysis and interpretation of the database supported by the proposed evaluation method gave insight into the geothermal conditions of the areas of interest.

The inclusion of abandoned hydrocarbon wells can support an increase in geothermal energy production in Hungary. This is an important objective in Hungary and may facilitate an increase in the share of renewables in the national energy mix (Tóth 2016). Currently, the direct utilization of geothermal energy has reached 1,000 MW_{th} capacity in Hungary. The proposed complex evaluation and

utilization of the abandoned hydrocarbon wells can help double this geothermal energy production rate in the next decade.

Funding Open access funding provided by University of Miskolc. The research was carried out with the support of the GINOP-2.3.2-15-2016-00010 “Development of enhanced engineering methods with the aim at utilization of subterranean energy resources” project of the Research Institute of Applied Earth Sciences of the University of Miskolc in the framework of the Széchenyi 2020 Plan, funded by the European Union, co-financed by the European Structural and Investment Funds.

Declarations

Conflict of interest On behalf of all authors, the corresponding author states that there is no conflict of interest.

Open Access This article is licensed under a Creative Commons Attribution 4.0 International License, which permits use, sharing, adaptation, distribution and reproduction in any medium or format, as long as you give appropriate credit to the original author(s) and the source, provide a link to the Creative Commons licence, and indicate if changes were made. The images or other third party material in this article are included in the article's Creative Commons licence, unless indicated otherwise in a credit line to the material. If material is not included in the article's Creative Commons licence and your intended use is not permitted by statutory regulation or exceeds the permitted use, you will need to obtain permission directly from the copyright holder. To view a copy of this licence, visit <http://creativecommons.org/licenses/by/4.0/>.

References

- Afzal P (2018) Comparing ordinary kriging and advanced inverse distance squared methods based on estimating coal deposits; case study: East-Parvardeh deposit, central Iran. *J Min Environ* 9(3):753–760. <https://doi.org/10.22044/jme.2018.6897.1522>
- Allen PA, Allen JR (2013) Basin analysis: principles and application to petroleum play assessment, 3rd edn. Wiley, Chichester, UK
- Arcanum (2019) A harmadidőszak korbeosztása [The age classification of the third period]. <https://www.arcanum.hu/hu/online-kiadvanyok/pannon-pannon-enciklopedia-1/magyarorszag-foldje-1d58/a-karpat-medence-foldtortenete-1fec/paleogen-retegtan-es-osfol-drajz-nagymarosy-andras-214a/a-harmadidoszak-korbeosztasa-214d/>. Accessed 3 Apr 2019
- Árpási M, Gy P, Andristyaká A (1997) Geothermal pilot projects on utilization of low-temperature reserves in Hungary. *Trans Geotherm Resour Counc* 21:327–330
- Babak O, Deutsch CV (2008) Statistical approach to inverse distance interpolation. *Stoch Env Res Risk A* 23:543–553. <https://doi.org/10.1007/s00477-008-0226-6>
- Barylo A (2000) Assessment of the energy potential of the Beregovsky Geothermal System, Ukraine. Report no. 3, Geothermal Training Program, Reykjavík, Iceland
- Békési E, Lenkey L, Limberger J, Porkoláb K, Balázs A, Bonté D, Vrijlandt M, Horváth F, Cloetingh S, Wees J (2017) Subsurface temperature model of the Hungarian part of the Pannonian Basin. *Glob Planet Chang* 171:48–64. <https://doi.org/10.1016/j.gloplacha.2017.09.020>
- Blahó J (2011) Object base Turbidite modelling of Demjén fields: applied technology and best practices. In: CEE Conference,

- Budapest, 17 November 2011, Society of Petroleum Engineer, Richardson, TX
- Bobok E, Tóth A (2007) First geothermal pilot power plant in Hungary. *Acta Montan Slov* 12:176–180
- Boldizsár T (1967) Terrestrial heat and geothermal resources in Hungary. *Bull Volcanol* 30:221–227
- Buday T, Szűcs P, Kozák M, Püspöki Z, McIntosh RW, Bódi E, Bálint B, Bulátkó K (2015) Sustainability aspects of thermal water production in the region of Hajdúszoboszló-Debrecen, Hungary. *Environ Earth Sci* 74:7511–7521. <https://doi.org/10.1007/s12665-014-3983-1>
- Cohen KM, Finney SC, Gibbard PL, Fan J-X (2013) The ICS International Chronostratigraphic Chart. *Episodes* 36:199–204. <https://doi.org/10.18814/epiiugs/2013/v36i3/002>
- Davis AP, Michaelides EE (2009) Geothermal power production from abandoned oil wells. *Energy* 34:866–872. <https://doi.org/10.1016/j.energy.2009.03.017>
- Deming D (1989) Application of bottom-hole temperature corrections in geothermal studies. *Geothermics* 18:775–786. [https://doi.org/10.1016/0375-6505\(89\)90106-5](https://doi.org/10.1016/0375-6505(89)90106-5)
- Dövényi Z (2016) A Kárpát-medence földrajza (Geography of the Carpathian Basin), Akadémiai Kiadó. <https://doi.org/10.1556/9789630598026>
- Dövényi P, Horváth F, Liebe P, Gálfi J, Erki I (1983) Geothermal conditions of Hungary. *Geophys Trans* 29(1):3–114
- Elias AS, Mock JC (2013) *Encyclopedia of Quaternary science*. Elsevier, Amsterdam
- Gazo FM (1992) Reservoir assessment of the Mak-Ban geothermal field, Luzon, Philippines. Report 6, UNU-GTP, UNU Iceland, pp1–32
- Gyollai I (2007) A pannon medence geodinamikai fejlődése a balatonfelvidéki granulit xenolitok példáján [Geodynamic development of the Pannonian basin on the example of granulite xenoliths in the Balaton Uplands]. Report, Eötvös Loránd Research Network, EARTO, Brussels
- Haás J (2013) *Geology of Hungary*. Springer, Berlin, 246 pp. <https://doi.org/10.1007/978-3-642-21910-8>
- Hantschel T, Kauerauf A (2009) *Fundamentals of basin and petroleum systems modelling*. Springer, Berlin, 476 pp. <https://doi.org/10.1007/978-3-540-72318-9>
- Horváth F (2007) A pannon medence geodinamikája (esztörténeti és geofizikai szintézis): akadémiai nagydoktori értekezés [Geodynamics of the Pannonian Basin (synthesis of the history of ideas and geophysics)]. PhD Thesis. http://geophysics.elte.hu/geofiz_tortenete/regebbi/Geofizika_tortenete_segedanyag.pdf. Accessed 19 July 2019
- Huismans RS, Podladchikov YY, Cloetingh S (2001) Dynamic modelling of the transition from passive to active rifting, application to the Pannonian Basin. *Tectonics* 20(6):1021–1039. <https://doi.org/10.1029/2001TC900010>
- Kai W, Bin Y, Guomin J, Xingru W (2018) A comprehensive review of geothermal energy extraction and utilization in oilfields. *J Pet Sci Eng* 168:465–477. <https://doi.org/10.1016/j.petrol.2018.05.012>
- Keveiné Bárány I (1992) The physical geography of the Bükk Mountains. *Abstracta Botanica* 16(2):75–86
- Lenkey L, Dövényi P, Horváth F, Cloetingh SAPL (2002) Geothermics of the Pannonian basin and its bearing on the neotectonics. EGU Stephan Mueller Special Publication Series 3, European Geosciences Union, Munich, Germany, pp 29–40
- Liu X, Falcone G, Alimonti C (2018) A systematic study of harnessing low temperature geothermal energy from oil and gas reservoirs. *Energy* 142:346–355. <https://doi.org/10.1016/j.energy.2017.10.058>
- MBFSZ (2017) MBFSZ MAP SERVER. <https://map.mbfisz.gov.hu>. Accessed 15 July 2018
- Mckenzie D (1978) Some remarks on the development of sedimentary basins. *Earth Planet Sci Lett* 40:25–32. [https://doi.org/10.1016/0012-821X\(78\)90071-7](https://doi.org/10.1016/0012-821X(78)90071-7)
- MFGI (2015) Hungary's thermal wells, vol VII (corrections). Hungarian Institute of Geology and Geophysics (MFGI), Budapest
- Miklós R, Darabos E, Lénárt L, Kovács A, Pelczéder Á, Szabó NP, Szűcs P (2020) Karst water resources and their complex utilization in the Bükk Mountains, northeast Hungary: an assessment from a hydrogeological perspective. *Hydrogeol J* 28:2159–2172. <https://doi.org/10.1007/s10040-020-02168-0>
- MND (2012) National Energy Strategy 2030. Ministry of National Development, Budapest. http://www.terport.hu/webfm_send/2658. Accessed 15 July 2018
- Nash MH, Daugherty LA, Wierenga PJ, Nance SA, Gutjahr A (1988) Horizontal and vertical kriging of soil properties along a transect in southern New Mexico. *Soil Sci Soc Am J* 52:1086. <https://doi.org/10.2136/sssaj1988.03615995005200040035>
- Nelskamp S, Verweij JM (2013) Using basin modeling for geothermal energy exploration in The Netherlands. Search and Discovery Article no. 120134, Posted March 13, 2013. Adapted from extended abstract prepared in conjunction with poster presentation at AAPG Hedberg Conference, AAPG2012, Petroleum Systems: Modeling The Past, Planning The Future, Nice, France, 1–5 October 2012
- Osipov VI (2015) The Terzaghi theory of effective stress. In: Physicochemical theory of effective stress in soils. SpringerBriefs in Earth Sciences. Springer, Cham, Switzerland. https://doi.org/10.1007/978-3-319-20639-4_2
- Pelikán P (ed) (2005) *Geology of the Bükk Mountains*. Mining and Geological Survey of Hungary, Budapest, Hungary
- Petrik A, Beke B, Fodor L, Lukács R (2016) Cenozoic structural evolution of the southwestern Bükk Mts. and the southern part of the Darnó Deformation Belt (NE Hungary). *Geol Carpath* 67(1):83–104. <https://doi.org/10.1515/geoca-2016-0005>
- Royden L, Horváth F, Nagymarosy A, Stegena L (1983) Evolution of the Pannonian Basin System: 2. subsidence and thermal history. *Tectonics* 2(1):91–137. <https://doi.org/10.1029/TC002i001p00091>
- Rybach L (1973) Warmeproduktionsbestimmungen an Gesteinen der Schweizer Alpen [Determinations of heat production in rocks of the Swiss Alps]. Beiträge zur Geologie der Schweiz. Geotechnische Serie 51, Kummerly & Frei, Bern, Switzerland, 43 pp
- Steiner F (1988) Most frequent value procedures (a short monograph). *Geophys Trans* 34:139–260
- Steiner F (1991) The most frequent value: introduction to a modern conception of statistics. Akadémiai Kiadó, Budapest
- Szabó NP, Balogh GP, Stickel J (2018) Most frequent value-based factor analysis of direct-push logging data. *Geophys Prospect* 66:530–548. <https://doi.org/10.1111/1365-2478.12573>
- Szanyi J, Kovács B (2010) Utilization of geothermal systems in South-East Hungary. *Geothermics* 39:357–364. <https://doi.org/10.1016/j.geothermics.2010.09.004>
- Sztrákos K (1973) Foraminifera fáciesek az Eger-Demjén környéki paleogénben [Foraminifera facies in the Paleogene around Eger-Demjén]. *Földtani Közlöny* 103:156–165
- Szűcs P (2017) Groundwater: an invisible part of the hydrological cycle (in Hungarian). *Magyar Tudomány* 178(10):1184–1197
- Szűcs P, Madarász T (2013) Hydrogeology in the Carpathian basin: how to proceed? *European Geologist* 35:17–20
- Szűcs P, Civan F, Virág M (2006) Applicability of the most frequent value method in groundwater modeling. *Hydrogeol J* 14:31–43
- Templeton JD, Ghoreishi-Madiseh SA, Hassani F, Al-Khawaja MJ (2014) Abandoned petroleum wells as sustainable sources of geothermal energy. *Energy* 70:366–373. <https://doi.org/10.1016/j.energy.2014.04.006>

- Timko DJ, Fertl WH (1972) How downhole temperatures, pressures affect drilling. *World Oil* 175(5):73–88
- Tóth A (2016) Magyarország geotermikus felmérése [Geothermal survey of Hungary]. Hungarian Energy and Public Utility Regulatory Authority, Budapest
- Tóth A (2017) Geothermal conditions of Zala County (in Hungarian). *Műszaki Földtudományi Közlemények* 86(2):180–187
- Turai E, Vurom B (2013) Applications of the IP method in the field of database protection, Proceedings of IX Carpathian Basin Environmental Science Conference, Miskolc, Hungary, June 2013, pp 237–242
- Ungerer P, Burrus J, Doligez B, Chenet PY, Bessis F (1990) Basin evaluation by integrated two-dimensional modeling of heat transfer, fluid flow, hydrocarbon generation, and migration. *AAPG Bull* 74:309–335
- VITUKI (1994) Thermal wells of Hungary, vol VI. VITUKI Rt., Budapest
- Vrsaljko D, Pavelić D, Miknić M, Brkić M, Kovačić M, Hećimović I, Hajek-Tadesse V, Avanić R, Kurtanjek N (2006) Middle Miocene (Upper Badenian/Sarmatian) Palaeoecology and evolution of the environments in the area of Medvednica Mt. (North Croatia). *Geol Croat* 59(1):51–63
- Wang K, Yuan B, Ji B, Wu X (2018) A comprehensive review of geothermal energy extraction and utilization in oilfields. *J Pet Sci Eng* 168:465–477. <https://doi.org/10.1016/j.petrol.2018.05.012>
- Wygrala BP (1989) Integrated study of an oil field in the southern Po basin, northern Italy. PhD Thesis, Ber Kernforschungsanlage Jülich, Jülich, Germany, 217 pp
- Xianbiao B, Weibin M, Huashan L (2012) Geothermal energy production utilizing abandoned oil and gas wells. *Renew Energy* 41:80–85. <https://doi.org/10.1016/j.renene.2011.10.009>
- Yi-Hwa EW, Ming-Chih H (2016) Comparison of spatial interpolation techniques using visualization and quantitative assessment. *Appl Spatial Statistics IntechOpen*. <https://doi.org/10.5772/65996>

Publisher's note Springer Nature remains neutral with regard to jurisdictional claims in published maps and institutional affiliations.